Hindawi Publishing Corporation
Journal of Nanomaterials
Volume 2015, Article ID 936482, 11 pages
http://dx.doi.org/10.1155/2015/936482

Hindawi

Research Article

Physical Properties of ZnO Thin Films Codoped with Titanium and Hydrogen Prepared by RF Magnetron Sputtering with Different Substrate Temperatures

Fang-Hsing Wang,[1] Jen-Chi Chao,[1] Han-Wen Liu,[1] and Tsung-Kuei Kang[2]

[1] *Department of Electrical Engineering and Graduate Institute of Optoelectronic Engineering, National Chung Hsing University, Taichung 40227, Taiwan*
[2] *Department of Electronic Engineering, Feng-Chia University, Taichung 40724, Taiwan*

Correspondence should be addressed to Fang-Hsing Wang; fansen@dragon.nchu.edu.tw

Received 11 November 2014; Accepted 22 December 2014

Academic Editor: Yibing Cai

Copyright © 2015 Fang-Hsing Wang et al. This is an open access article distributed under the Creative Commons Attribution License, which permits unrestricted use, distribution, and reproduction in any medium, provided the original work is properly cited.

Transparent conducting titanium-doped zinc oxide (TZO) thin films were prepared on glass substrates by RF magnetron sputtering using 1.5 wt% TiO_2-doped ZnO as the target. Electrical, structural, and optical properties of films were investigated as a function of $H_2/(Ar + H_2)$ flow ratios (R_H) and substrate temperatures (T_S). The optimal R_H value for achieving high conducting TZO:H thin film decreased from 10% to 1% when T_S increased from RT to 300°C. The lowest resistivity of 9.2×10^{-4} Ω-cm was obtained as $T_S = 100$°C and $R_H = 7.5$%. X-ray diffraction patterns showed that all of TZO:H films had a hexagonal wurtzite structure with a preferred orientation in the (002) direction. Atomic force microscopy analysis revealed that the film surface roughness increased with increasing R_H. The average visible transmittance decreased with increasing R_H for the RT-deposited film, while it had not considerably changed with different R_H for the 300°C-deposited films. The optical bandgap increased as R_H increased, which is consistent with the Burstein-Moss effect. The figure of merits indicated that $T_S = 100$°C and $R_H = 7.5$% were optimal conditions for TZO thin films as transparent conducting electrode applications.

1. Introduction

Transparent conducting oxide (TCO) films were widely used in optoelectronic devices such as low-emissivity windows, electromagnetic shielding, gas sensors, information displays, and photovoltaic cells [1–5]. Indium tin oxide (ITO) is a commonly used TCO at present, but indium is a rare metal and with toxicity. Zinc oxide (ZnO) is regarded as a promising TCO material due to its advantages such as nontoxicity, abundance, and high stability in hydrogen plasma [1]. Since undoped ZnO films have an unstable electrical conductivity, group IIIA element (Al, Ga, or In) doped ZnO thin films have been widely studied to enhance the film conductivity [3–8]. A few reports suggest that Ti is a possible dopant for ZnO films because Ti is a quadrivalent cation and has a radius of 68 pm which is close to that of Zn (74 pm) [9–11]. The quadrivalent cation may provide one more valence than the trivalent cation as it substitutes Zn in ZnO films. TZO thin films have been prepared by several techniques, including radio frequency (RF)/DC sputtering [11–13], chemical vapor deposition (CVD) [14], and sol-gel process [15]. Among these methods, sputtering has advantages such as good uniformity, high process controllability, and large-area deposition and has been widely used. Lin et al. investigated the effect of Ti content on the properties of Ti-doped ZnO (TZO) films [9]. Chung et al. investigated the effect of the TiO_2 content of the target, the working pressure, and the substrate temperature on the properties of TiO_2-doped ZnO films [10]. In our previous research, effects of thickness and plasma treatment on the properties of Ti-doped ZnO films had been investigated [11, 16].

Recently, the density functional theory proposed by van de Walle shows that hydrogen atoms can act as donors

and thus enhance electrical conductivity of ZnO [17, 18]. In addition, experimental investigates on effects of in situ hydrogen doping on ZnO-related films have been performed [5, 12, 19, 20]. Lee et al. reported that hydrogen might act like an anionic dopant by binding with oxygen in Al-doped ZnO (AZO) films [19]. Das and Ray investigated AZO films prepared by RF magnetron sputtering under $Ar + H_2$ ambient and concluded that the low resistivity (4.5×10^{-4} Ω-cm) was achieved at the substrate temperature of 300°C with the $H_2/(Ar + H_2)$ flow ratio of 10% [20].

In this study, TZO thin films were prepared by RF magnetron sputtering under various $H_2/(Ar + H_2)$ ratios in sputtering ambient at different substrate temperatures. The temperature dependent effects of hydrogen doping on the electrical, structural, and optical properties of TZO thin films were investigated.

2. Experimental Procedures

TZO powder (ZnO = 98.5 wt%, 99.999% purity; TiO_2 = 1.5 wt%, 99.99% purity) was calcined at 1400°C to prepare ceramic targets with a 2 inch diameter. Before the deposition process, the glass substrates were cleaned ultrasonically with isopropyl alcohol and deionized water and subsequently dried under a blown nitrogen gas. TZO thin films with a thickness of about 330 nm were deposited on 30 mm × 30 mm × 2 mm Corning 1737 glass substrates by using a Syskey 13.56 MHz RF magnetron sputtering system at a constant power of 100 W. The working distance was 10 cm. The base pressure of the deposition chamber was below 5×10^{-6} Torr and the working pressure was maintained at 5×10^{-3} Torr in Ar or $Ar + H_2$ mixture gas with a constant flow rate of 20 sccm. A series of TZO films were prepared with varying the $H_2/(Ar + H_2)$ flow ratio from 0% to 15% at various substrate temperatures ranging from room temperature (RT) to 300°C. The substrate holder rotated at a constant speed of 35 rpm during sputtering to obtain a better film uniformity.

Film thickness was measured using a spectroscopic ellipsometer (nanoview, SEMF-100) and confirmed by field emission scanning electron microscopy (FE-SEM) (JEOL, JSM-6700). Crystallographic phases and crystalline quality of films were analyzed using X-ray diffraction (XRD) (PANalytical, 18 kW rotating anode X-ray generator, Japan) with *Cu-K*α radiation (λ = 0.154056 nm) in the conventional $\vartheta - 2\vartheta$ mode. Morphology of films was observed using FE-SEM and atomic force microscopy (AFM) (Digital Instrument, NS4/D3100CL/Multimode). Electrical resistivity, carrier concentration, and Hall mobility were determined by a four-point probe (Napson RT-70/RG-5) and Hall-effect measurements (Ecopia, HMS-3000) using the van der Pauw method at a magnetic field of 0.55 T. The optical transmittance spectrum was measured using a UV/VIS/IR spectrophotometer (Jasco, V-570) in the 220–2500 nm wavelength range. The chemical bonding states of elements in TZO films were investigated using an X-ray photoelectron spectroscopy (XPS) (ULVAC-PHI, PHI 5000 Versaprobe). All measurements were performed at RT.

3. Results and Discussion

Figure 1 exhibits the variation in the resistivity, Hall mobility, and carrier concentration of TZO thin films with $H_2/(Ar + H_2)$ gas flow ratio (R_H) and substrate temperature (T_S). At the lower T_S of RT-100°C, it was found that the electrical properties of TZO films strongly depended on R_H. As R_H varied from 0% to 15%, the resistivity of RT-deposited films ranged between 1.08 and 1.82×10^{-3} Ω-cm, which differed by near three orders of magnitude. However, the dependence of the electrical properties on R_H became relatively small as T_S increased to above 200°C. The resistivity of films deposited at 300°C ranged between 3.47×10^{-3} and 2.07×10^{-3} Ω-cm. Besides, the resistivity of TZO thin films initially decreased with increasing R_H and then increased with increasing R_H despite substrate temperatures. The optimal electrical property is obtained with the lowest film resistivity. The lowest resistivities of TZO thin films deposited at RT, 100°C, 200°C, and 300°C were achieved when R_H were 10%, 7.5%, 5%, and 1%, respectively. These results reveal that electrical properties of TZO:H thin films strongly depend on T_S as well as hydrogen doping effect. Effectiveness of hydrogen doping in TZO films decreases with increasing T_S. Among these four T_S conditions, the lowest resistivity of 9.2×10^{-4} Ω-cm was achieved for the film deposited at 100°C with R_H = 7.5% and accompanied by a carrier concentration of 8.49×10^{20} cm^{-3} and a mobility of 7.95 cm^2/V-s. The decrease in resistivity can be due to the increase in carrier concentration (n) and/or in mobility (μ). From Figure 1, it was found that the lower-T_S deposited TZO films had more n and μ dependence on R_H. In addition, the decrease in film resistivity was mainly due to the increase in carrier concentration. For the 100°C-deposited films, the carrier concentration increases by more than 2 orders of magnitude, that is, from 7.5×10^{18} (R_H = 0%) to 8.5×10^{20} cm^{-3} (R_H = 7.5%), while the Hall mobility increases only by about 2.6 times of magnitude (from 3.6 to 9.3 cm^2/V-s). For the 300°C deposited films, the decrease of the resistivity (R_H = 1.0%) completely results from the increase of the carrier concentration even though the Hall mobility decreases. These results reveal that the hydrogen doping is more effective in generating free carriers at a lower substrate temperature.

As mentioned above, the variation trends of the carrier concentration and the Hall mobility with different R_H depend on the T_S. In the earlier literatures, Bikowski and Ellmer performed the ZnO:Al and ZnMgO:Al film depositions in Ar/H_2 ambient (R_H = 0–10%) at RT and 300°C [21]. Their results showed that the resistivity decreased by about 2 orders of magnitude for the RT deposition, while resistivity increased for the 300°C depositions with increasing hydrogen flow. Kim et al. performed the ZnO:Ga film depositions at 80–270°C and observed the optimal resistivities obtained with R_H = 6%, 10%, and 0% at T_S = 80°C, 160°C, and 270°C, respectively [22]. Their minimum resistivities and corresponding R_H values are comparatively different from our results due to different doped cation and deposition parameters. van de Walle theoretically studied the role of hydrogen in ZnO through a first principles investigation, based on density functional theory, and produced strong evidence that hydrogen could

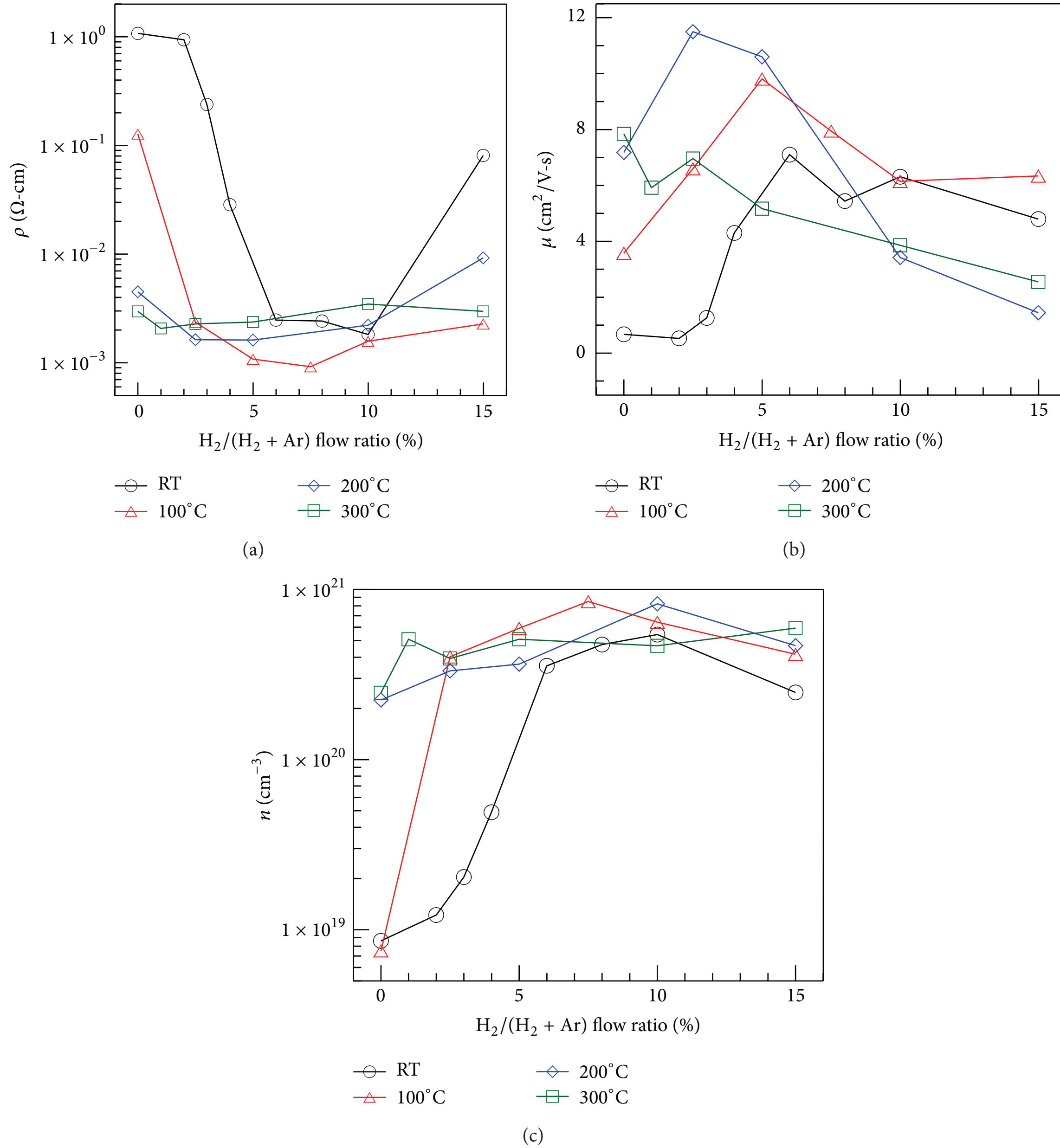

Figure 1: Dependence of the (a) resistivity, (b) Hall mobility, and (c) carrier concentration of TZO thin films on $H_2/(Ar + H_2)$ flow ratio and substrate temperature.

incorporate in high concentrations and acted as a shallow donor to enhance film conductivity [17, 18]. In this work, the lower deposition temperature causes worse crystallinity and more defects in the film. Thus, effectiveness of hydrogen doping can be enhanced at low T_S by inserting into interstitial (H_i) or in oxygen bond-center (H_O) lattice sites. Besides, it is possible that hydrogen extracts oxygen from thin films, causing the formation of oxygen vacancy and interstitial zinc atoms to increase the carrier concentration [23, 24]. With further increasing R_H beyond the abovementioned optimal value, film resistivity started to increase due to the decreased Hall mobility. R. B. H. Tahar and N. B. H. Tahar indicated that the mobility was dominant by neutral and ionized impurity scattering in ZnO films [25]. Here, excess hydrogen doping may generate more defects and free carriers, which enhance carrier scattering phenomenon, thus causing the decrease of Hall mobility. It is also noted that Hall mobility has a maximum value at the middle substrate temperature (200°C). Lin et al. proposed that oxygen atoms tended to create more neutral impurity scattering centers in the low and high temperature range, and hence Hall mobility was degraded [26].

Figure 2 shows the relationship between Hall mobility (μ) and carrier concentration (n) for the TZO thin films prepared at RT and 300°C. For the films deposited at the low temperature (RT), the Hall mobility increased with

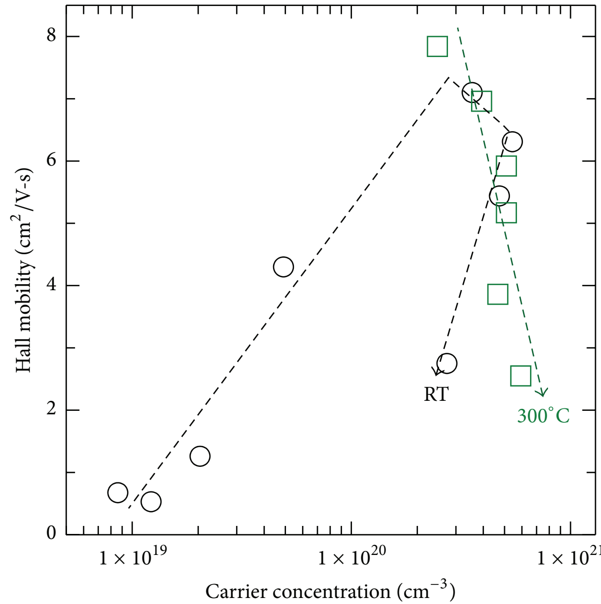

Figure 2: Relationship between Hall mobility (μ) and carrier concentration (n) for TZO thin films prepared at RT and 300°C.

the carrier concentration as R_H ranges from 0 to 6%. This increase suggests that carrier transport in the films with less than 6% R_H (i.e., $n < 2 \times 10^{20}\,\text{cm}^{-3}$) is limited by grain boundary scattering, which assumes that potential barriers at grain boundaries limit the carrier transport significantly. As the R_H increased from 6% to 8%, the Hall mobility decreased with the carrier concentration, revealing that ionized impurity scattering dominated due to the increase of electron scattering centers [27]. This behavior is consistent with the theoretical prediction by Brooks-Herring theory [28]. With further increasing R_H more than 8% (i.e., $n > 6 \times 10^{20}\,\text{cm}^{-3}$), both the mobility and the carrier concentration decreased, indicating that grain boundary scattering became prominent in carrier transport processes. It is thought that high hydrogen contents restrain grain growth, resulting in poor crystallinity and small grain size. The Hall mobility-carrier concentration relationship has also been reported in sputtered AZO and GZO thin films [21, 22]. Electron transport mechanism depends on carrier concentration and is explained by a combined model of ionized-impurity scattering or grain barrier scattering for the low-temperature deposited films. The carrier concentration of the 300°C-deposited films ranged between 2 and $6 \times 10^{20}\,\text{cm}^{-3}$ and the decrease of the Hall mobility is accompanied with the increase of the carrier concentration with increasing R_H, indicating the ionized impurity scattering dominates at the high substrate temperature. Bikowski and Ellmer have revealed that 300°C-deposited AZO films exhibited the ionized impurity scattering [21], while Kim et al. have related 270°C-deposited GZO films to grain barrier scattering [22]. The difference between this study and earlier research is not clear and may be due to different doped cations and process parameters.

XPS analysis was executed to explore the film composition and chemical states of elements in TZO thin films for clarifying the conducting mechanism. Figure 3(a) shows the XPS spectrum of the RT-deposited TZO thin film with R_H = 0%. Observed characteristic peaks in Figure 3(a) indicated that Ti existed in the thin films. The peaks located at around 530 nm are assigned to O 1s. Figures 3(b) and 3(c) show the spectra of O 1s for RT-deposited TZO thin films with R_H = 0% and 10%, respectively. The O 1s peak was asymmetric and could be resolved into three components, which were located at 530.1 (peak 1), 530.9 (peak 2), and 532.1 (peak 3) eV, respectively. The peak 1 can be attributed to O^{2-} ions in Zn–O bonds. The peaks 2 and 3 are ascribed to oxygen vacancy and loosely bound oxygen species (e.g., H_2O, O_2, and −OH) chemisorbed on the surface and grain boundary, respectively [4, 29]. To compare the characteristic peaks in Figures 3(b) and 3(c), the area ratio of the peak 2 apparently increased from 59% to 72%, indicating an increase in oxygen vacancies in the films. This result contributes to the increase of the carrier concentration in the H_2-doped TZO thin films. The area ratio of the peak 1 decreased from 26% to 13%, indicating a decrease in the amount of oxygen atoms in a fully stoichiometric Zn-O surrounding. It is thought that hydrogen may react with oxygen to form hydroxides in sputtering ambient, causing the lack of oxygen in the films.

Figures 4(a) and 4(b) exhibit the XRD spectra of TZO thin films deposited at different substrate temperatures with R_H = 0% and 10%, respectively. All patterns exhibited only a (0 0 2) preferential orientation along the c-axis at diffraction angles (2θ) near 34°, indicating a hexagonal wurtzite structure, and no characteristic peak of TiO_2 was found. The (0 0 2) peak intensity increased with increasing T_S, suggesting that the film crystallinity was enhanced at a high temperature regardless of hydrogen addition. The enhanced film crystallinity is due to an increase in the surface diffusion of the adsorbed species with increasing T_S [4, 30]. Besides,

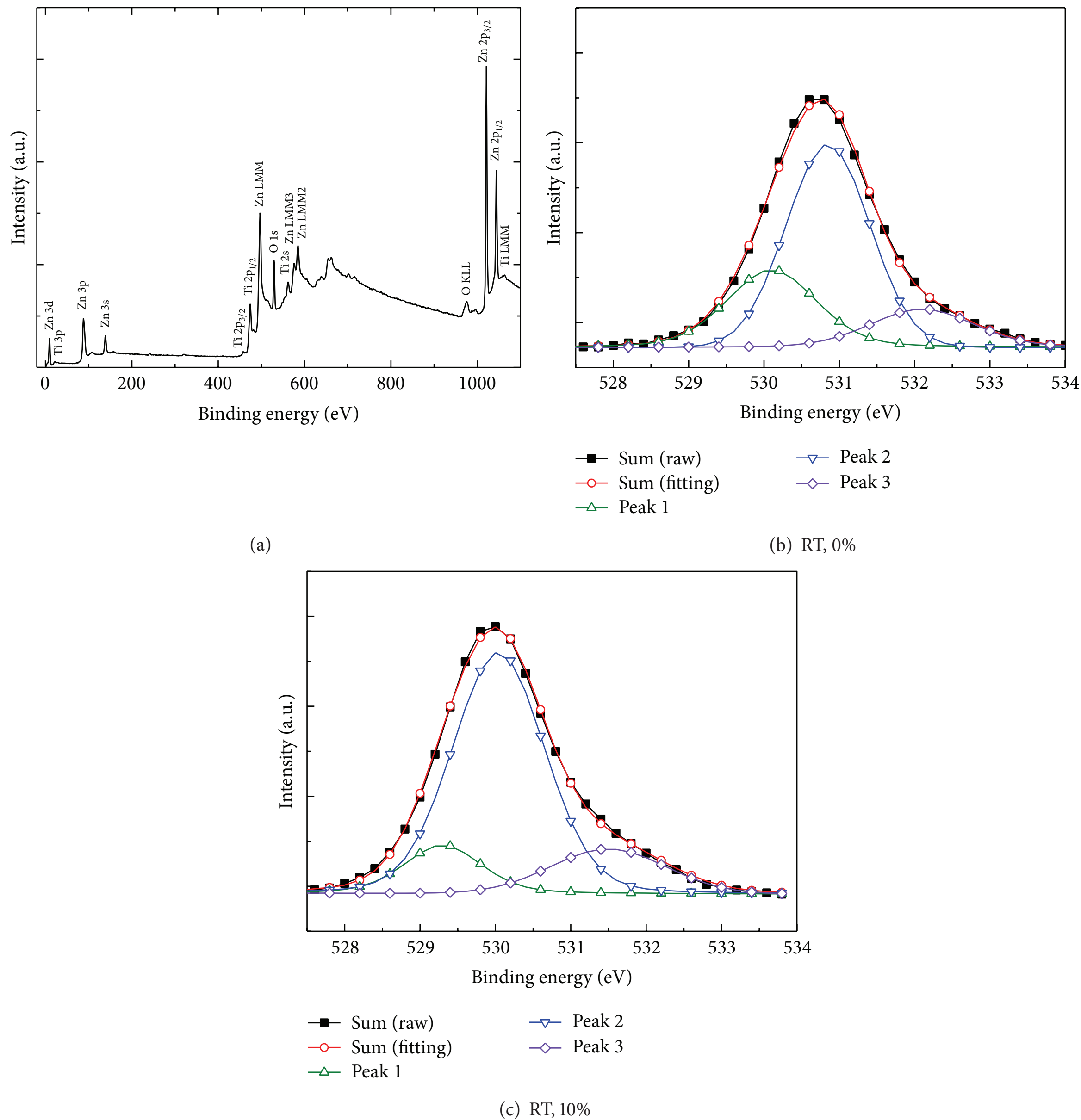

Figure 3: (a) XPS spectrum of the RT-deposited TZO thin film with R_H = 0%, and the XPS spectra of O 1s for RT-deposited TZO thin films with (b) R_H = 0% and (c) R_H =10%.

the (0 0 2) peak positions shifted toward larger diffraction angles as the T_S increased from RT to 300°C. This phenomenon indicates a decrease in the interplanar distance (d_{002}), which may be attributed to the fact that more Ti atoms replace substitutional Zn atoms at a higher T_S. Since the ionic radius of Ti^{4+} (68 pm) is smaller than that of Zn^{2+} (74 pm), the position of the (0 0 2) peak is expected to shift to a large 2θ value. Figures 4(c) and 4(d) show the XRD spectra of TZO films deposited at RT and 300°C, respectively, with various R_H. For the RT depositions (see Figure 3(c)), the increased R_H resulted in a noticeable decrease in peak intensity, revealing the fact that hydrogen incorporated into the films and degraded the film crystallinity. Besides, it was found that the 2θ peak shifted toward lower diffraction angle, indicating an expansion of crystal lattice [17]. It is believed that hydrogen atoms may situate in the center of Zn–O bonds, parallel to the c-axis which would lead to an increase in the lattice parameter of the films. At the high T_S (see Figure 4(d)), the variations of (0 0 2) peak intensities of TZO films with various R_H were relatively small as compared to those at RT. The positions of all diffraction peaks did not obviously changed and were at 34.33 ± 0.03°. It indicated that the structure of the 300°C-deposited TZO film did not considerably change with increasing R_H. This result also explains why the electrical properties of the 300°C-deposited TZO films have no significant variation for different R_H.

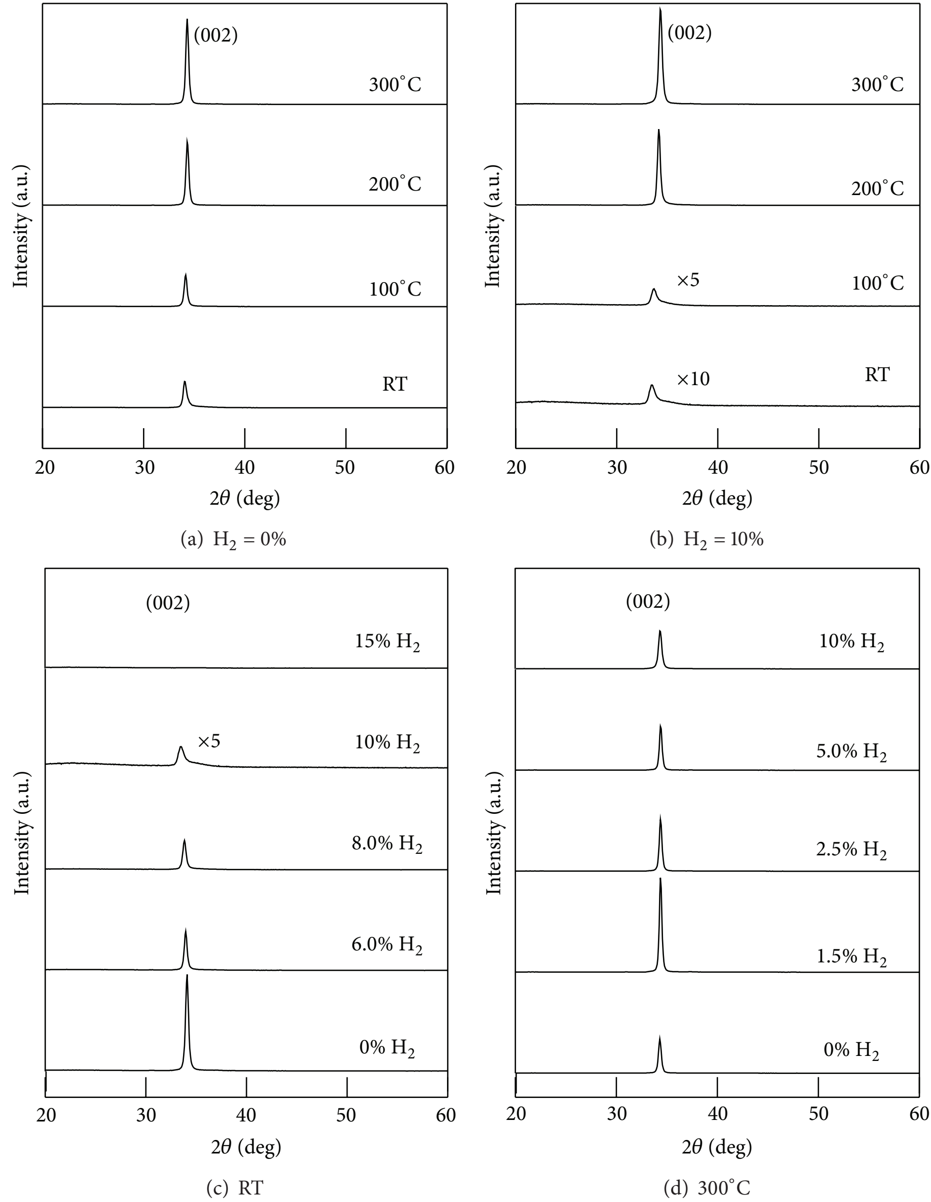

Figure 4: XRD spectra of TZO thin films deposited with H_2/(Ar + H_2) flow ratio of (a) 0% and (b) 10% at various substrate temperatures and with various H_2/(Ar + H_2) flow ratios at (c) RT and (d) 300°C.

Figure 5(a) shows the full-width at half-maximum (FWHM) and grain size of TZO thin films deposited with R_H = 0 and 10% at various T_S. The grain size was estimated with Scherrer's formula [31]:

$$D = \frac{0.94\lambda}{\beta \cos\theta}, \quad (1)$$

where λ = 0.154056 nm, D is grain size, and β is FWHM. The FWHM decreased with the increase of the T_S regardless of hydrogen content, indicating the increase of the grain size. Lin et al. also reported the similar trend in the 50–200°C-deposited AZO films [32]. Besides, the nonhydrogenated TZO films exhibited larger grain sizes than those deposited with R_H = 10% regardless of T_S. Figure 5(b) shows the FWHM and grain size of TZO films deposited at RT and 300°C with various R_H. A small addition of hydrogen could increase the grain size, while excess hydrogen would deteriorate film crystallinity and thus decrease the grain size.

Figures 6(a)–6(f) display the 45°-tilted FE-SEM images of TZO thin films deposited at RT and 300°C with R_H = 0, 5%, and 10%. The cross-section views of TZO films showed a well-defined columnar structure. Comparing the RT and 300°C-deposited films, it was found that the latter has a smoother surface morphology and a denser columnar structure than the former. This is due to the fact that the high substrate temperature increases the energy of adsorbed

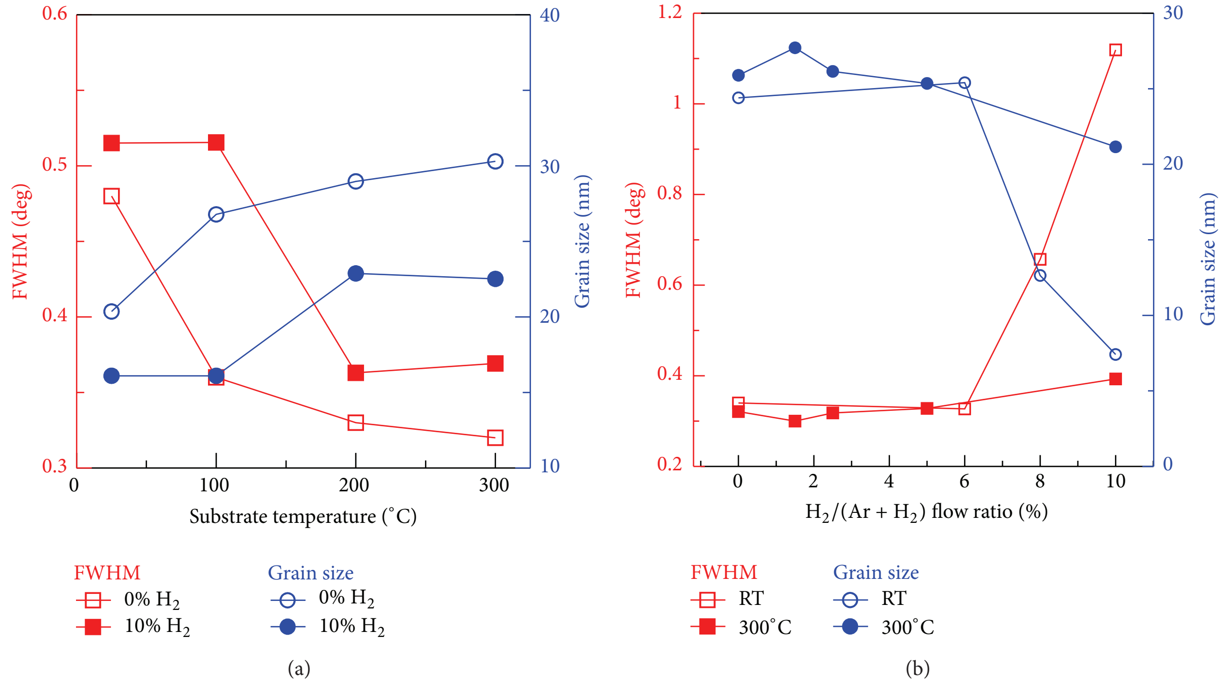

Figure 5: Full-width at half-maximum (FWHM) and grain size of TZO thin films deposited (a) with $H_2/(Ar + H_2)$ flow ratio of 0 and 10% at various substrate temperatures and (b) with various $H_2/(Ar + H_2)$ flow ratios at RT and 300°C.

ions and thus improves the structural properties of TZO films, which is consistent with the XRD results shown in Figure 4. Comparing the films with different R_H, the surface morphology of TZO films became spherical shaped domains and rough with increasing R_H. Addonizio et al. and Lee also reported that the surface of AZO films became rough as hydrogen added in sputtering gas [33, 34]. However, Gottardi et al. indicated that the ZnO films deposited in pure Ar ambient showed a rougher surface than that prepared in Ar + H_2(10%) ambient. In this work, the estimated mean-free path of energetic particles at RT would be around 1.6 cm, which is smaller than the working distance (10 cm). Hydrogen dilution in sputtering gas may decrease the scattering cross-section and hence increase the energy of the sputtering particles. Besides, hydrogen has strong reduction and etching effect on film surface. It is believed that enhanced Ar^+ bombardment and strong reduction and etching effect of hydrogen on film surfaces disturbs the grain growth and results in the rough surface. The AFM images of TZO thin films (see Figure 7) exhibited that the RMS roughness increased from 1.99 to 4.79 nm as R_H increased from 0 to 7.5%.

Figures 8(a) and 8(b) show the optical transmittance spectra of TZO thin films prepared with various R_H at T_S = RT and 300°C, respectively, in the wavelength region of 220–2500 nm. All TZO films showed sharp absorption edges in the ultraviolet range and a decreased transmittance with R_H in the near infrared (NIR) region. The decreasing transmittance in the NIR region with wavelength can be explained by the classical Drude model [35], which indicates that the decrease of transmittance is attributed to free carrier absorption that increases with the hydrogen incorporation. Variations of the average visible transmittance (T_{ave}) (including glass substrate) in the 400–750 nm region are shown in Figure 9(a). The T_{ave} slightly decreased from 84.0% to 81.7% as the R_H varied from 0 to 10% for the RT-deposited films, while T_{ave} remained around 84.7% ± 0.5% for those prepared at 300°C. Furthermore, T_{ave} significantly decreased to 70.5% as for the film with very high R_H (20%). The lower visible transmittance at the lower T_S can be attributed to the enhancement of scattering and absorption of light due to worse crystallinity and a rougher film surface, as the XRD and SEM analyses show. This similar behavior on AZO thin films was reported by our group and Liu et al. [4, 27]. The findings indicated that the AZO thin film prepared with relative high H_2-flow rate showed bad transparency due to the increase of intergranular zinc atoms caused by hydrogen doping.

Figure 9(b) presents the optical bandgap (E_g) of TZO thin films prepared with different R_H at the T_S = RT and 300°C. The E_g was determined by taking the energy corresponding to the maximum of $d\alpha^2/d(h\nu)$, where α is the optical absorption coefficient calculated from the transmittance spectra and $h\nu$ is the photon energy [36]. The calculated E_g of the RT-prepared films increased from 3.29 to 3.61 eV as R_H increased from 0 to 10% and then decreased to 3.57 eV for a further increase in R_H (20%). The E_g broadening phenomenon is known as the Burstein-Moss effect, which specifies the Fermi level inside the conduction band that moves upward with increasing carrier concentration due to the filling of conduction band by the increase of electron carriers [37]. The film deposited at the higher temperature (300°C) exhibited

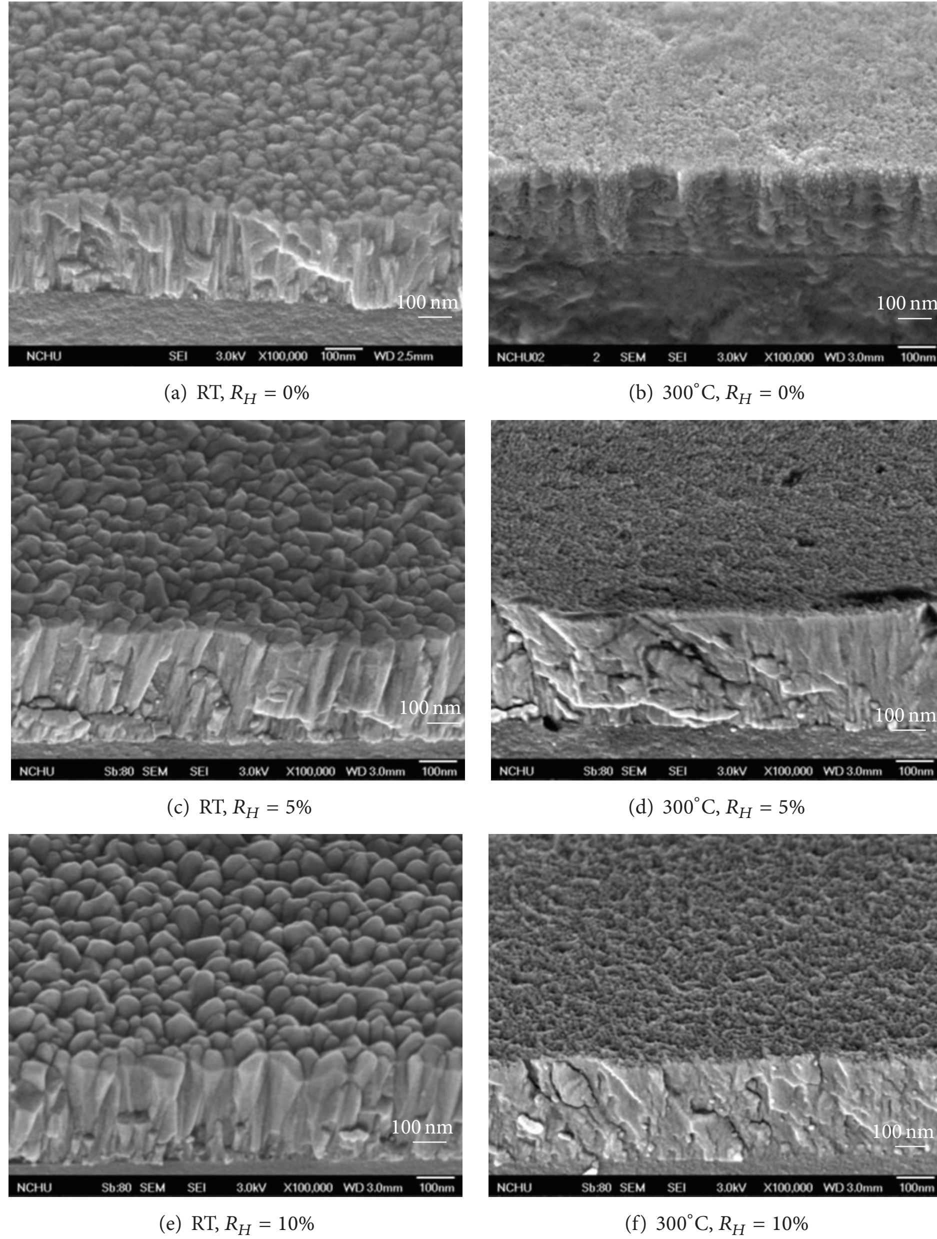

(a) RT, $R_H = 0\%$

(b) 300°C, $R_H = 0\%$

(c) RT, $R_H = 5\%$

(d) 300°C, $R_H = 5\%$

(e) RT, $R_H = 10\%$

(f) 300°C, $R_H = 10\%$

Figure 6: FE-SEM images of TZO thin films deposited at RT and 300°C with $R_H = 0$, 5%, and 10%.

a weak dependence of E_g on R_H and their E_g increased from 3.43 to 3.53 eV as the R_H increased from 0 to 10%. This weak dependent for the 300°C-deposited films is attributed to the behavior that less hydrogen atoms are doped in the TZO films.

The transparent conducting thin films must have low resistivity and high optical transparency for the application of solar cells. A way for evaluating this compromise is by means of figure of merit (FOM). FOM defined by Haacke is one of the important indices for judging the effectiveness of different processes. FOM is defined by [38]

$$\text{FOM}\left(\Omega^{-1}\right) = \frac{T^{10}}{R_S}, \quad (2)$$

where T is the average visible transmittance and R_S is the sheet resistance of films. Figure 10 shows the FOM of TZO films deposited with different substrate temperatures and $H_2/(Ar + H_2)$ flow ratios. At the high T_S (200-300°C), FOM slightly increased for a small addition of H_2 and then decreased as R_H went beyond 2.5%. By contrast, FOM of the low T_S (RT-100°C) prepared films significantly increased over two orders of magnitude with increasing R_H and the highest FOM, $4.74 \times 10^{-3}\ \Omega^{-1}$, was achieved for the films prepared at 100°C with $R_H = 7.5\%$. These results indicate that the in situ hydrogen doping effectively improves electrooptical properties of TZO thin films and the effectiveness of hydrogen doping is strongly dependent on substrate temperature and $H_2/(Ar + H_2)$ flow ratio.

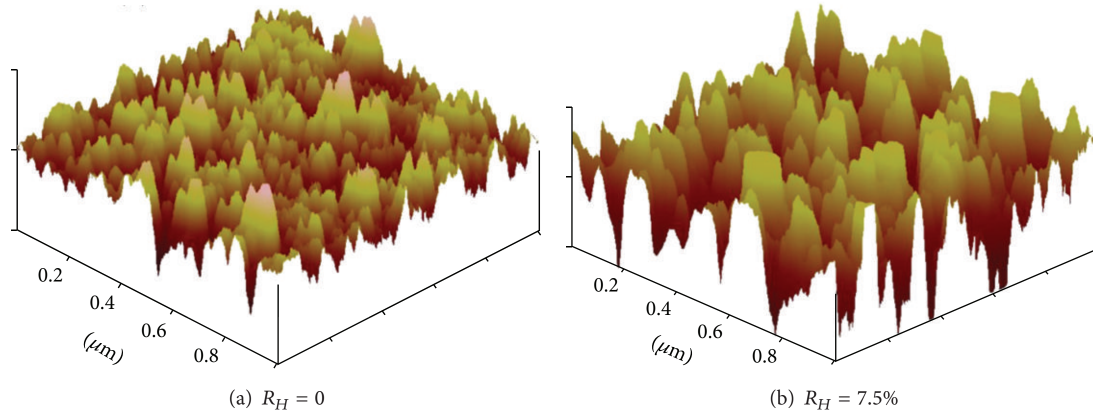

(a) $R_H = 0$ (b) $R_H = 7.5\%$

FIGURE 7: AFM images of TZO thin films (1 μm × 1 μm area) deposited at 100°C with $R_H = 0$ and 7.5%.

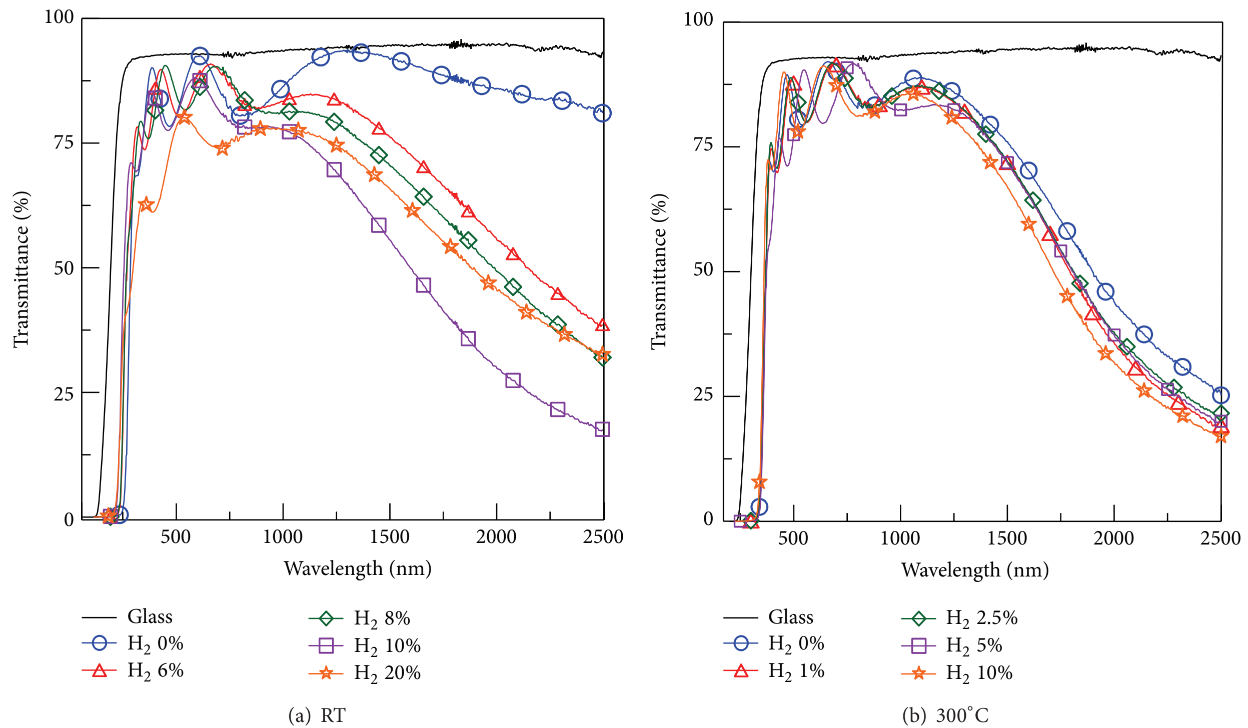

(a) RT (b) 300°C

FIGURE 8: Optical transmittance spectra of TZO thin films prepared with various $H_2/(Ar + H_2)$ flow ratios at substrate temperatures of (a) RT and (b) 300°C in the wavelength region of 220–2500 nm.

4. Conclusions

The hydrogen and titanium codoped ZnO thin films were fabricated by sputtering of a ZnO target containing 1.5 wt% TiO_2 in Ar/H_2 gas mixtures at substrate temperatures of RT-300°C on glass substrates. The XRD analysis showed that all of TZO films exhibit a (002) preferential orientation along the *c*-axis at $2\theta \sim 34^{\circ}$. The (002) peak shifted toward the large diffraction angles with increasing substrate temperature. The excess hydrogen addition in the TZO films resulted in the decrease of the (002) peak intensity and the left-shift of the peak position, revealing poor crystallinity due to that the hydrogen atoms might insert into the Zn–O bonds and extract oxygen from the film. The hydrogen incorporation in the TZO films improved the electrical and optical properties and the extent of improvement was dependent on the $H_2/(Ar + H_2)$ flow ratio along with the substrate temperature. The calculated Haacke's figure of merits showed that the optimized TZO films were achieved at the substrate temperature of 100°C and the $H_2/(Ar + H_2)$ flow ratio of 7.5% and accompanied by the resistivity of 9.2×10^{-4} Ω-cm and the average transmittance more than 80%. Excess hydrogen content deteriorated the electrooptical properties of the TZO films due to the poor crystallinity, the rough film surface, and the more defects

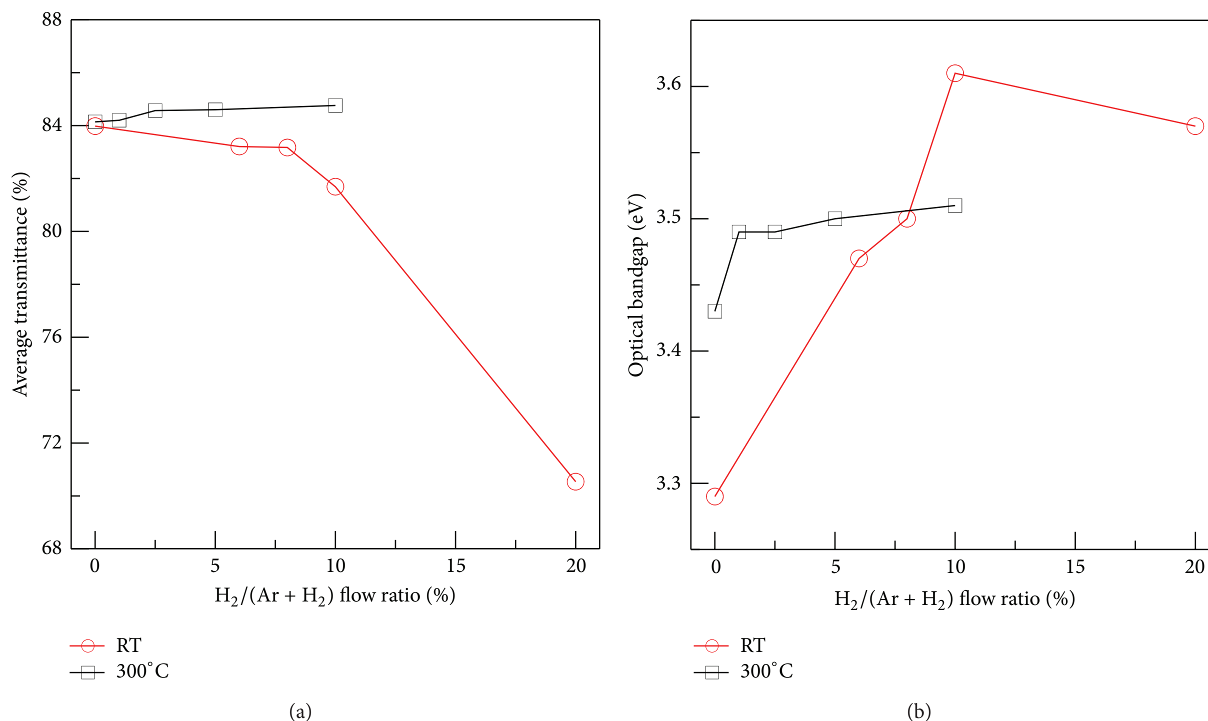

FIGURE 9: (a) Average transmittance and (b) optical bandgap of TZO thin films with different $H_2/(Ar + H_2)$ flow ratios.

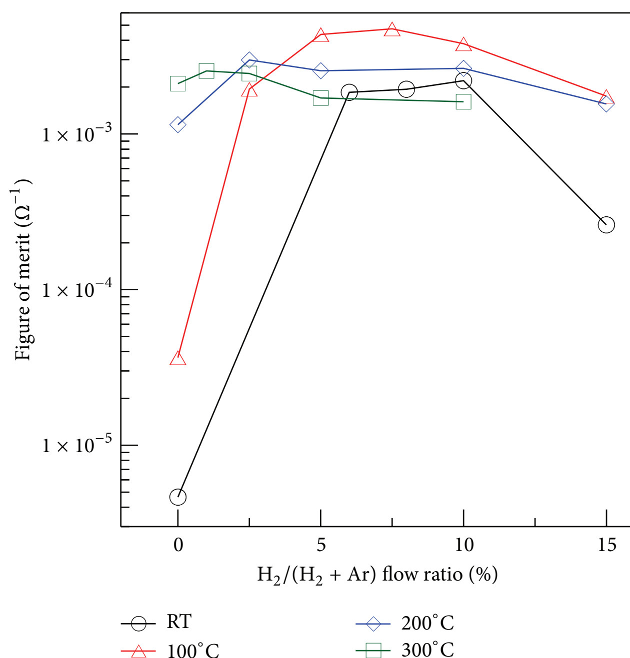

FIGURE 10: Figure of merit of TZO thin films deposited with different substrate temperatures and $H_2/(Ar + H_2)$ flow ratios.

in the films. The developed hydrogen and titanium codoped ZnO thin films have potential for transparent conducting electrode applications.

Conflict of Interests

The authors declare that there is no conflict of interests regarding to the publication of this paper.

Acknowledgments

This work has received financial support from the National Science Council of the Republic of China (Taiwan) under Contract no. NSC 101-2221-E-005-065. Authors thank Dr. Chia-Cheng Huang and Dr. Hung-Peng Chang for performing some measurements.

References

[1] H. C. Weller, R. H. Mauch, and G. H. Bauer, "Studies on the interface between novel type ZnO and p-a-SiC:H in 1.5 eV a-SiGe:H pin diodes in comparison to SnO_x and ITO," *Solar Energy Materials and Solar Cells*, vol. 27, no. 3, pp. 217–231, 1992.

[2] D. S. Ginley and C. Bright, "Transparent conducting oxides," *MRS Bulletin*, vol. 25, no. 8, pp. 15–18, 2000.

[3] T. Minami and T. Miyata, "Present status and future prospects for development of non- or reduced-indium transparent conducting oxide thin films," *Thin Solid Films*, vol. 517, no. 4, pp. 1474–1477, 2008.

[4] F.-H. Wang, H.-P. Chang, C.-C. Tseng, and C.-C. Huang, "Effects of H_2 plasma treatment on properties of ZnO:Al thin films prepared by RF magnetron sputtering," *Surface and Coatings Technology*, vol. 205, no. 23-24, pp. 5269–5277, 2011.

[5] P. K. Song, M. Watanabe, M. Kon, A. Mitsui, and Y. Shigesato, "Electrical and optical properties of gallium-doped zinc oxide

films deposited by dc magnetron sputtering," *Thin Solid Films*, vol. 411, no. 1, pp. 82–86, 2002.

[6] L. Cao, L. Zhu, J. Jiang, R. Zhao, Z. Ye, and B. Zhao, "Highly transparent and conducting fluorine-doped ZnO thin films prepared by pulsed laser deposition," *Solar Energy Materials and Solar Cells*, vol. 95, no. 3, pp. 894–898, 2011.

[7] S. H. Park, J. B. Park, and P. K. Song, "Characteristics of Al-doped, Ga-doped and In-doped zinc-oxide films as transparent conducting electrodes in organic light-emitting diodes," *Current Applied Physics*, vol. 10, no. 3, supplement, pp. S488–S490, 2010.

[8] T. Prasada Rao and M. C. Santhosh Kumar, "Physical properties of Ga-doped ZnO thin films by spray pyrolysis," *Journal of Alloys and Compounds*, vol. 506, no. 2, pp. 788–793, 2010.

[9] S. S. Lin, J. L. Huang, and P. Šajgalik, "The properties of Ti-doped ZnO films deposited by simultaneous RF and DC magnetron sputtering," *Surface and Coatings Technology*, vol. 191, no. 2-3, pp. 286–292, 2005.

[10] J. L. Chung, J. C. Chen, and C. J. Tseng, "The influence of titanium on the properties of zinc oxide films deposited by radio frequency magnetron sputtering," *Applied Surface Science*, vol. 254, no. 9, pp. 2615–2620, 2008.

[11] H.-P. Chang, F.-H. Wang, J.-C. Chao, C.-C. Huang, and H.-W. Liu, "Effects of thickness and annealing on the properties of Ti-doped ZnO films by radio frequency magnetron sputtering," *Current Applied Physics*, vol. 11, no. 1, supplement, pp. S185–S190, 2011.

[12] J. N. Duenow, T. A. Gessert, D. M. Wood, D. L. Young, and T. J. Coutts, "Effects of hydrogen content in sputtering ambient on ZnO:Al electrical properties," *Journal of Non-Crystalline Solids*, vol. 354, no. 19–25, pp. 2787–2790, 2008.

[13] Y. R. Park, J. Kim, and Y. S. Kim, "Effect of hydrogen doping in ZnO thin films by pulsed DC magnetron sputtering," *Applied Surface Science*, vol. 255, no. 22, pp. 9010–9014, 2009.

[14] J. Hu and R. G. Gordon, "Textured aluminum–doped zinc oxide thin films from atmospheric pressure chemical–vapor deposition," *Journal of Applied Physics*, vol. 71, pp. 880–890, 1992.

[15] F. Furusaki, J. Takahashi, and K. Kodaira, "Preparation of ITO thin films by sol-gel method," *Journal of the Ceramic Society of Japan*, vol. 102, no. 1182, pp. 200–205, 1994.

[16] F. H. Wang, H. P. Chang, and J. C. Chao, "Improved properties of Ti-doped ZnO thin films by hydrogen plasma treatment," *Thin Solid Films*, vol. 519, no. 15, pp. 5178–5182, 2011.

[17] C. G. van de Walle, "Hydrogen as a cause of doping in zinc oxide," *Physical Review Letters*, vol. 85, no. 5, pp. 1012–1015, 2000.

[18] C. G. van de Walle and J. Neugebauer, "Universal alignment of hydrogen levels in semiconductors, insulators and solutions," *Nature*, vol. 423, no. 6940, pp. 626–628, 2003.

[19] S. H. Lee, T. S. Lee, K. S. Lee, B. Cheong, Y. D. Kim, and W. M. Kim, "Characteristics of hydrogen co-doped ZnO: Al thin films," *Journal of Physics D: Applied Physics*, vol. 41, no. 9, Article ID 095303, 2008.

[20] R. Das and S. Ray, "Zinc oxide—a transparent, conducting IR-reflector prepared by rf-magnetron sputtering," *Journal of Physics D: Applied Physics*, vol. 36, no. 2, pp. 152–155, 2003.

[21] A. Bikowski and K. Ellmer, "Electrical transport in hydrogen-aluminium Co-doped ZnO and $Zn_{1-x}Mg_xO$ films: relation to film structure and composition," *Journal of Applied Physics*, vol. 113, no. 5, Article ID 053710, 2013.

[22] D.-H. Kim, S.-H. Lee, G.-H. Lee et al., "Effects of deposition temperature on the effectiveness of hydrogen doping in Ga-doped ZnO thin films," *Journal of Applied Physics*, vol. 108, no. 2, Article ID 023520, 2010.

[23] W. F. Liu, G. T. Du, Y. F. Sun et al., "Effects of hydrogen flux on the properties of Al-doped ZnO films sputtered in Ar + H_2 ambient at low temperature," *Applied Surface Science*, vol. 253, no. 6, pp. 2999–3003, 2007.

[24] J. F. Chang, W. C. Lin, and M. H. Hon, "Effects of post-annealing on the structure and properties of Al-doped zinc oxide films," *Applied Surface Science*, vol. 183, no. 1-2, pp. 18–25, 2001.

[25] R. B. H. Tahar and N. B. H. Tahar, "Mechanism of carrier transport in aluminum-doped zinc oxide," *Journal of Applied Physics*, vol. 92, no. 8, pp. 4498–4501, 2002.

[26] S. S. Lin, J. L. Huang, and P. Šajgalik, "Effects of substrate temperature on the properties of heavily Al-doped ZnO films by simultaneous r.f. and d.c. magnetron sputtering," *Surface and Coatings Technology*, vol. 190, no. 1, pp. 39–47, 2005.

[27] W. F. Liu, G. T. Du, Y. F. Sun et al., "Al-doped ZnO thin films deposited by reactive frequency magnetron sputtering: H_2-induced property changes," *Thin Solid Films*, vol. 515, no. 5, pp. 3057–3060, 2007.

[28] T. Minami, H. Sato, K. Ohashi, T. Tomofuji, and S. Takata, "Conduction mechanism of highly conductive and transparent zinc oxide thin films prepared by magnetron sputtering," *Journal of Crystal Growth*, vol. 117, no. 1–4, pp. 370–374, 1992.

[29] M. Chen, X. Wang, Y. H. Yu et al., "X-ray photoelectron spectroscopy and auger electron spectroscopy studies of Al-doped ZnO films," *Applied Surface Science*, vol. 158, no. 1-2, pp. 134–140, 2000.

[30] K. H. Kim, K. C. Park, and D. Y. Ma, "Structural, electrical and optical properties of aluminum doped zinc oxide films prepared by radio frequency magnetron sputtering," *Journal of Applied Physics*, vol. 81, no. 12, pp. 7764–7772, 1997.

[31] B. D. Cullity and S. R. Stock, *Elements of X-Ray Diffraction*, Prentice Hall, 3rd edition, 2001.

[32] S.-S. Lin, J.-L. Huang, and D.-F. Lii, "Effect of substrate temperature on the properties of Ti-doped ZnO films by simultaneous rf and dc magnetron sputtering," *Materials Chemistry and Physics*, vol. 90, no. 1, pp. 22–30, 2005.

[33] M. L. Addonizio, A. Antonaia, G. Cantele, and C. Privato, "Transport mechanisms of RF sputtered Al-doped ZnO films by H_2 process gas dilution," *Thin Solid Films*, vol. 349, no. 1, pp. 93–99, 1999.

[34] J.-H. Lee, "Effects of hydrogen incorporation and heat treatment on the properties of ZnO:Al films deposited on polymer substrate for flexible solar cell applications," *Current Applied Physics*, vol. 10, no. 3, supplement, pp. S515–S519, 2010.

[35] H. L. Hartnagel, A. L. Dawar, A. K. Jain, and C. Jagadish, in *Semiconducting Transparent Thin Films*, Institute of Physics Publishing, Bristol, UK, 1st edition, 1995.

[36] M. Purica, E. Budianu, E. Rusu, M. Danila, and R. Gavrila, "Optical and structural investigation of ZnO thin films prepared by chemical vapor deposition (CVD)," *Thin Solid Films*, vol. 403-404, pp. 485–488, 2002.

[37] E. Burstein, "Anomalous optical absorption limit in InSb," *Physical Review*, vol. 93, no. 3, pp. 632–633, 1954.

[38] G. Haacke, "New figure of merit for transparent conductors," *Journal of Applied Physics*, vol. 47, no. 9, pp. 4086–4089, 1976.

Journal of
Nanotechnology

International Journal of
Corrosion

International Journal of
Polymer Science
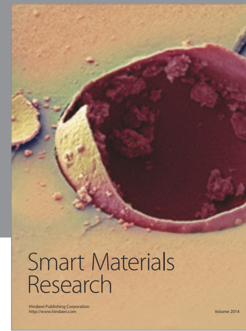
Smart Materials
Research

Journal of
Composites

BioMed
Research International

Hindawi
Submit your manuscripts at
http://www.hindawi.com
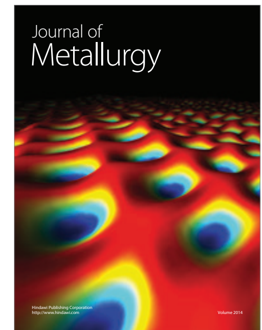
Journal of
Metallurgy

Journal of
Materials
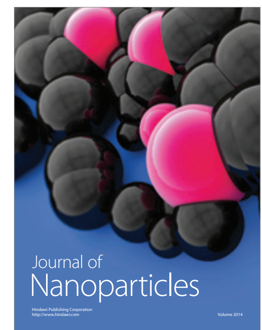
Journal of
Nanoparticles
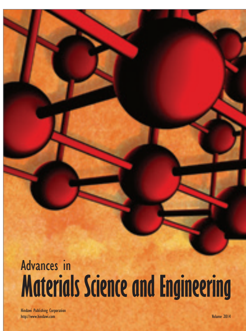
Advances in
Materials Science and Engineering

Scientifica
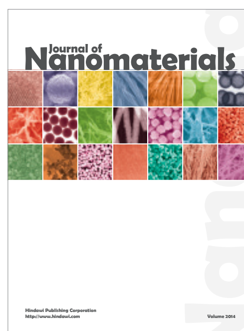
Journal of
Nanomaterials
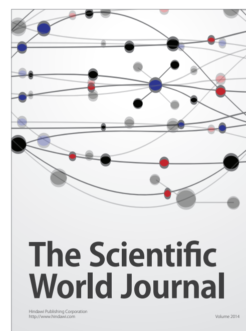
The Scientific
World Journal
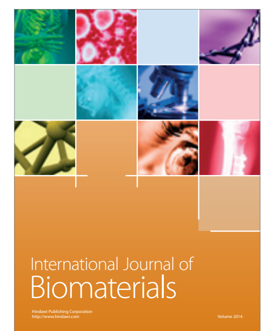
International Journal of
Biomaterials

Journal of
Nanoscience

Journal of
Coatings

Journal of
Crystallography

Journal of
Ceramics
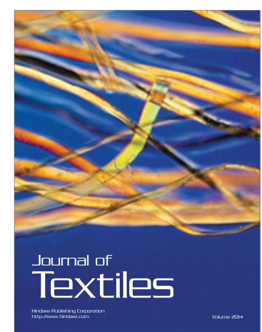
Journal of
Textiles